Publications of the Astronomical Society of the Pacific, **119**: 1063–1068, 2007 September

A Coronagraph Based on Stepped-Transmission Filters

Deqing Ren[1,2] and Yongtian Zhu[1]
Received 2007 April 3; accepted 2007 July 31; published 2007 September 12

ABSTRACT. We propose a coronagraph for direct imaging of Earth-like planets orbiting nearby bright stars. The coronagraph is based on an apodization pupil composed of two stepped-transmission filters. We show that the coronagraph can achieve 10^{-10} high-contrast imaging at an angular distance larger than (2–3)λ/D theoretically. The employment of the stepped-transmission filters significantly simplifies the manufacturing of the transmission pupil, making it possible to be used for high-contrast imaging in practice.

1. INTRODUCTION

Discovering life on another planet will potentially be one of the most important scientific advances of this century. The search for life requires the ability to detect photons directly from planets and the use of spectroscopy to analyze physical and atmospheric conditions. The direct detection of Earth-like low-mass planets is, however, extremely challenging. For NASA's *Terrestrial Planet Finder Coronagraph* (*TPF-C*), a contrast of 10^{-10} at an angular distance better than $4\lambda/D$ is required.

Many high-contrast imaging coronagraphs have been proposed recently (see the review by Guyon et al. 2006) which can theoretically achieve 10^{-10} contrast at a few λ/D from a bright star. Among them is the transmission pupil apodization (Nisenson & Papaliolios 2001; Aime et al. 2002; Gonsalves & Nisenson 2003). Traditional transmission pupil apodization uses a continuous variation transmission function to modulate the intensity on the pupil, and high-contrast imaging can be achieved by using the prolate spheroidal functions (Aime et al. 2002). A problem for such a continuous variation function is the difficulty of manufacturing the pupil apodization mask, since the transmission needs to be controlled at every position in the pupil with high degree of precision. To overcome this problem, we propose an apodization pupil that deploys only stepped-transmission filters in which the intensity is apodized with a finite number of steps of identical transmission in each step. Since the transmission needs to be controlled in finite steps only, it significantly simplifies the manufacturing of the apodization pupil, making it possible to be used for high-contrast imaging.

2. PRINCIPLE OF THE STEPPED-TRANSMISSION APODIZATION

The configuration of the coronagraph of the stepped-transmission pupil apodization is the same as those of the conventional apodized pupils. The stepped-transmission filters that serve as the pupil apodization masks are located in the collimated beam. Star and planet light is modulated by the pupil masks, and the associated images are formed on the coronagraph focal plane by a camera lens. For a stepped-transmission filter, the amplitude of the electric field is variable between different steps. However, it is constant in each step. Figure 1 shows the distribution of the transmission amplitude of a stepped-transmission filter. For a square aperture, we assume that the size of each side is L, and the aperture is divided into n zones, where n is an odd integer. The width of each zone is w, with $w \le L/n$. In the case $w = L/n$, the filter has no gap between two adjacent steps and therefore delivers higher transmission than that with a gap (i.e., $w < L/n$). At step k the amplitude is expressed as $p(k)$, where $k = 0, \pm 1, \pm 2, \ldots, \pm(n-1)/2$. For the case in which there is no gap between two adjacent steps, the complex amplitude of electric field for a stepped-transmission filter on the pupil expressed as a function of k is

$$t(k) = [\mathrm{rect}(k) * \mathrm{comb}(k)]\left[p(k)\,\mathrm{rect}\left(\frac{k}{n}\right)\right]. \qquad (1)$$

In the coronagraph focal plane, the complex amplitude of the electric field is the Fourier transform of the complex amplitude of the pupil. For a coronagraph that is composed of one stepped-transmission filter, the focal plane complex amplitude of the electric wave can be expressed as

$$T(u) = (n)\,[\mathrm{sinc}(u)\ \mathrm{comb}(u)] * [P(u) * \mathrm{sinc}(nu)], \qquad (2)$$

where $P(u)$ is the Fourier transform function of $p(k)$. In the above equation, the first part, $[\mathrm{sinc}(u)\ \mathrm{comb}(u)]$, is a comb function, and its frequency is determined by the comb function. However, the amplitude of the comb function is modulated by

[1] National Astronomical Observatories/Nanjing Institute of Astronomical Optics and Technology, Chinese Academy of Sciences, Nanjing, China.
[2] Physics and Astronomy Department, California State University, Northridge, CA; ren.deqing@csun.edu.

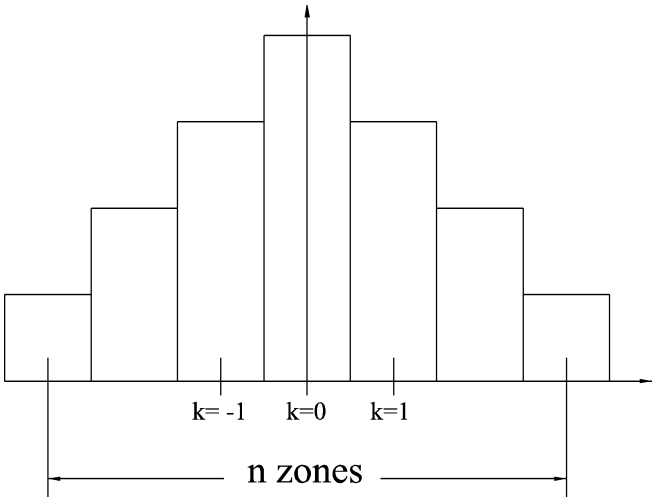

FIG. 1.—Transmission amplitude distribution of a stepped-transmission filter.

the sinc(u) function. A high-density sampling (i.e., a large n) will result in a large peak-peak distance of the comb function on the image plane. The second part, [$P(u) * \text{sinc}(nu)$], is the convolution of $P(u)$ and sinc(nu). The component sinc(nu) is the Fourier transform of the full pupil aperture, where the component $P(u)$ is the Fourier transform of a discrete function that determined how much contrast an apodization pupil can achieve. As the result of the convolution, sinc(nu) is slightly broadened, but its amplitude outside the point-spread function (PSF) disk can be depressed by $P(u)$. The second part is very similar to that of the conventional transmission apodization pupil. As a result of the convolution of the two parts, $T(u)$ appears to have many small peaks whose positions are determined by the comb function. At the PSF center, the center peak has a maximum value, while other peaks have smaller values that are functions of u. Since the intensity of the PSF in the focal plane is the square of $T(u)$, by finding the optimized function $p(k)$ the PSF can achieve maximum contrast at a specific angular distance.

The function $p(k)$ is critical to achieving high-contrast imaging at an angular distance a few λ/D away. It is known that the prolate spheroidal function (Slepian 1964) is an optimal solution that achieves this goal by maximally concentrated energy around zero frequency in the frequency domain. Recently, it was also used for the optimal design of different coronagraphs of apodized pupil (Aime et al. 2002; Kasdin et al. 2003). For our apodized pupil, since we only use a finite number of transmission steps, we should use the discrete prolate spheroidal function (DPSF; Verma et al. 1996; Slepian 1978; Eberhard 1973). The DPSF allows the use of an apodized pupil with a finite number of transmission steps while maximizing the energy concentration in the PSF central disk and thus maximizing the contrast in the discovery area.

The apodized pupil is composed of two identical stepped-transmission filters, one after another with 90° orientation. One filter provides apodization in the u-direction, while the other provides apodization in the vertical v-direction. The two filters therefore provide two-direction apodization and can be expressed as

$$T(u, v) = (n^2)\,\{[\text{sinc}(u)\,\text{comb}(u)] * [P(u) * \text{sinc}(nu)]\} \times\{[\text{sinc}(v)\,\text{comb}(v)] * [P(v) * \text{sinc}(nv)]\}. \quad (3)$$

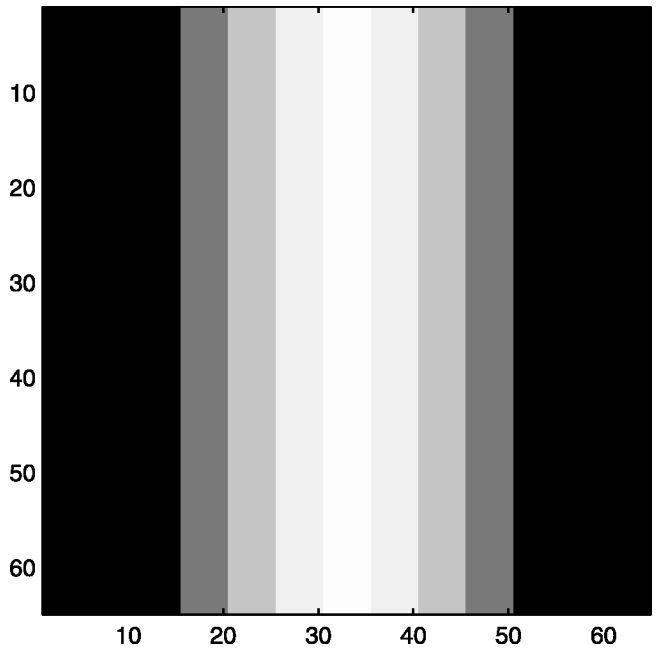

FIG. 2.—Transmission amplitude pattern of a 13 step filter.

Although one filter could be used for the apodized pupil, a pupil with two filters delivers better contrast, since the PSF is apodized in two directions. The outer working angular distance of the two-filter coronagraph is limited by the step number of the filter, and is roughly equal to λ/D times the step number of the filter.

3. NUMERICAL SIMULATIONS

To demonstrate the coronagraph's performance for high-contrast imaging, numerical simulation for a two-filter apodized pupil is performed by using Matlab. Each filter has 13 steps. Figure 2 shows the transmission amplitude pattern of the filter, in which each step has the same transmission and is sampled by several pixels. The PSF of the associated two-filter apodized pupil is shown in Figure 3. The PSF section plot along the diagonal direction is shown in Figure 4. The PSF of the associated square aperture without apodization is also plotted for comparison. The apodization pupil, with a transmission of 13%, can achieve a contrast of 10^{-10} at an angular distance larger than $\sim 2\lambda/D$ compared with the nonapodized square pupil. The

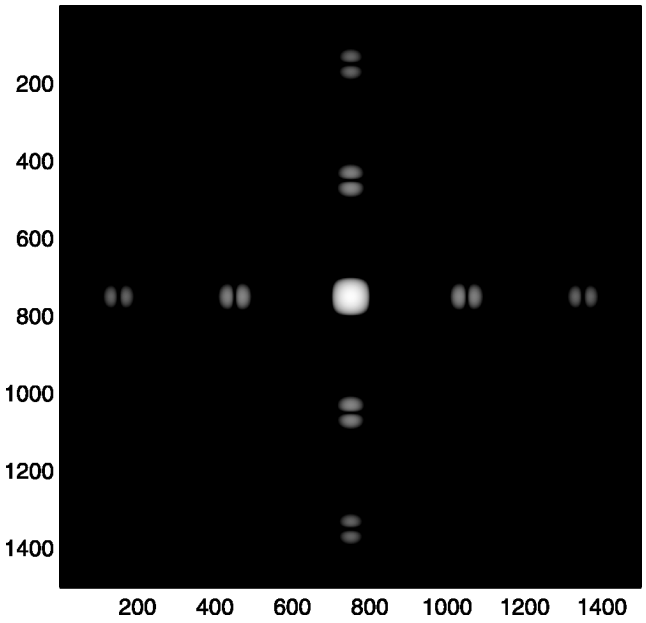

FIG. 3.—PSF of the 13 step apodization pupil. The intensity is in logarithmic scale.

second diffraction peak is located at an angular distance that is equal to λ/D times the step number of the filter (see Fig. 4). For the 13 step filters, it is $13\lambda/D$, which limits its outer working angular distance to $10.5\lambda/D$. Figure 5 shows the PSF contour map with the intensity higher than 10^{-10}. The discovery area, defined as the area with an intensity lower than 10^{-10}, is cut off as many separate squares by grids of high intensity.

Ultra–high-contrast imaging, in which the intensity in most

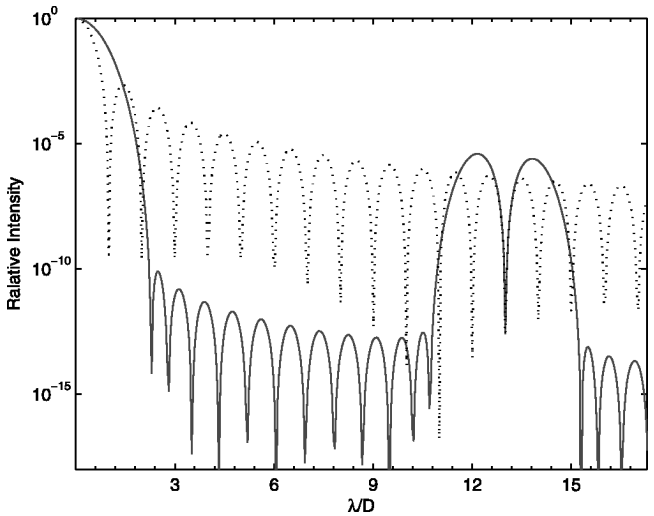

FIG. 4.—PSF section plot of the 13 step apodization pupil (*solid line*) designed for high-contrast imaging. The dotted line shows the PSF of the squared pupil without apodization. The plots are cut along the square diagonal direction.

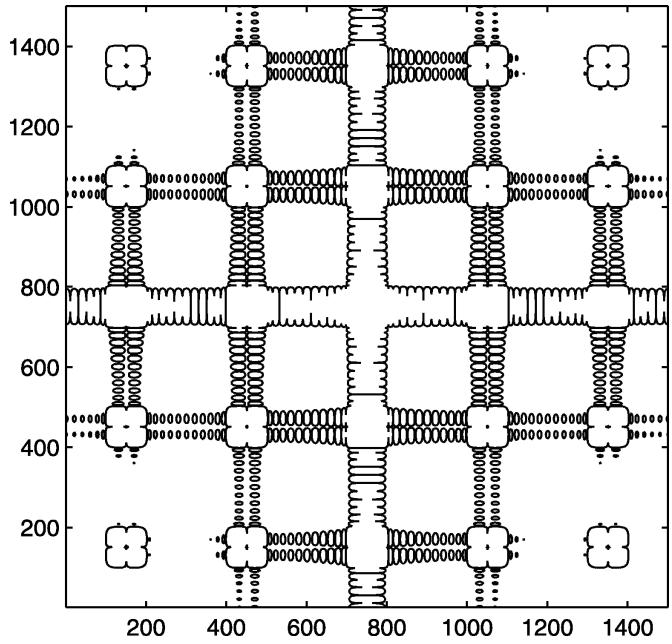

FIG. 5.—PSF contour of the 13 step apodization pupil designed for high-contrast imaging.

of the discovery area is significantly lower than 10^{-10}, can also be achieved by using the stepped-transmission filter technique. Figure 6 shows the PSF section plot for the apodized pupil with the 13 stepped-transmission filters that are designed for ultra–high-contrast imaging. With 9% transmission, it achieves $\sim 10^{-14}$ ultrahigh contrast at an angle larger than $3\lambda/D$ along the diagonal direction. Figure 7 shows the PSF contour map

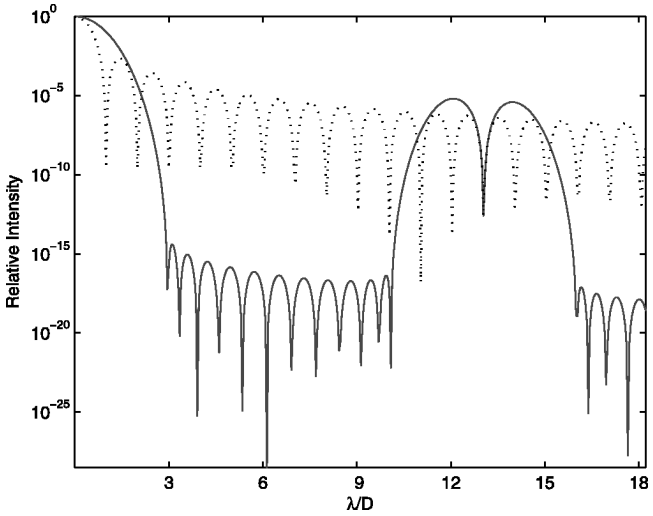

FIG. 6.—PSF section plot of the 13 step apodization pupil (*solid line*) designed for ultra–high-contrast imaging. The dotted line shows the PSF of the squared pupil without apodization. The plots are cut along the square diagonal direction.

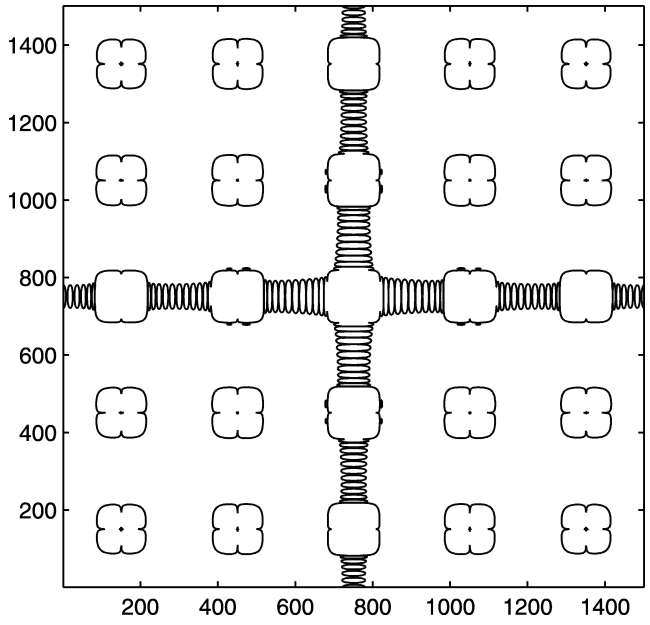

FIG. 7.—PSF contour of the 13 step apodization pupil designed for ultra–high-contrast imaging.

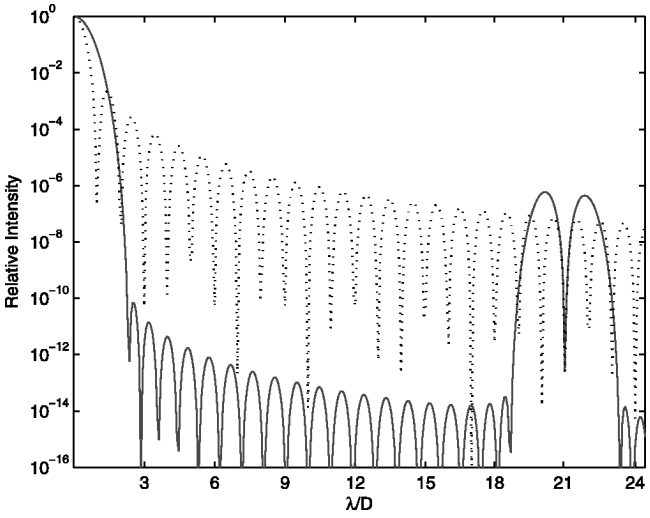

FIG. 8.—PSF section plot of the 21 step apodization pupil (*solid line*) designed for high-contrast imaging. The dotted line shows the PSF of the squared pupil without apodization. The plots are cut along the square diagonal direction.

with intensity higher than 10^{-10}. The high intensity cross divides the discovery area into four large pieces, in which isolated islands of high intensity are located. Compared with Fig. 5, the ultra–high-contrast design increases the discovery area, since the grids of high intensity are efficiently depressed.

As discussed, for high-contrast imaging increasing the step number of transmission filters can increase the outer working angle. Figure 8 shows the PSF section plot along the diagonal direction for the apodized pupil with 21 step filters. Again, it can achieve a contrast of 10^{-10} at an angular distance larger than $\sim 3\lambda/D$. The transmission is 13% for the two-filter pupil. As expected, the second diffraction peak is located at $21\lambda/D$, and it achieves an outer working angle of $\sim 19\lambda/D$. The 21 step filters can also be designed for ultra–high-contrast imaging.

4. DISCUSSION AND COMPARISON WITH OTHER TECHNIQUES

The PSF pattern of the stepped-transmission pupil is very similar to that of the checkerboard pupil proposed by Vanderbei et al. (2004), and both can deliver 10^{-10} high contrast at an angular distance larger than $\sim 3\lambda/D$. However, the PSF energy distributions of the two pupils are different. For the checkerboard mask, the Airy throughput, which is defined as the light contained in the central diffraction spot, is 50% of the total mask throughput (Vanderbei et al. 2004). There is a factor of ~2 difference between the mask throughput and the Airy throughput useful for detection (Guyon et al. 2006). The remaining 50% of the light is located outside the discovery area and behaves as unwanted scattered light. As discussed by Guyon et al. (2006), a high Airy throughput against the total mask throughput is important for planet detection in a zodiacal or exozodiacal background.

For the stepped-transmission pupil, the Airy throughput takes ~99% of the total pupil throughput for both masks with 13 and 21 steps. This efficiently minimizes scattering of zodiacal and exozodiacal light induced by the coronagraph.

The checkerboard pupil is a binary mask. That is, the transmission is modulated as 0 or 1 in the pupil. A significant advantage of such a mask is its achromatism for broadband imaging. For moderate contrast such as 10^{-7}, the checkerboard is easy to manufacture. Recently, checkerboard masks optimized for 10^{-7} contrast imaging were reported and manufactured (Enya et al. 2007). However, for 10^{-10} high-contrast imaging, the manufacturing of the checkerboard mask is challenging, since the open slits at or near the mask edge may be too narrow to manufacture precisely for a reasonable mask size.

The stepped transmission pupil can be realized by using the neutral-density filter technique. Neutral-density filters uniformly attenuate the intensity of light over a broad spectral range. Traditionally, uncoated, gray tinted glass is used to attenuate the light by absorption, and this technique is called absorption glass neutral-density attenuation (AGNDA). The degree of attenuation is determined by the thickness of the glass. Recently, metallic-coated neutral-density attenuation (MCNDA) has been developed and is commercially mature. For MCNDA, the attenuation is achieved by a combination of reflection and absorption of thin metallic coating. The dominated error source for a transmission filter is the transmission accuracy. Currently, transmission precision of 5% of the nominal value is achievable with standard manufacturing procedure.

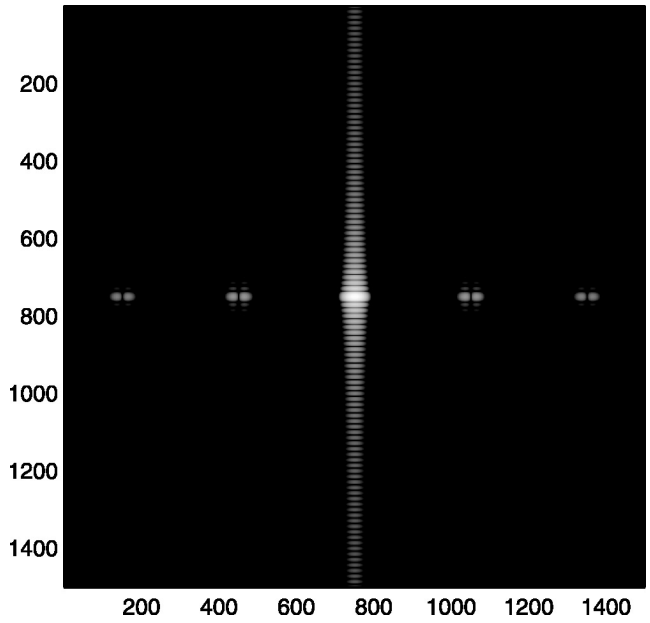

FIG. 9.—PSF of a 21 step one-filter apodization pupil. The intensity is in logarithmic scale.

We expect that 2% precision may be achievable by improving the current procedure (with the goal of 1% precision). The 2% transmission error degrades the contrast on the order of 10^{-2} to 10^{-3}. In this case, an ultra–high-contrast system designed for the error-free case can compensate the transmission error and deliver a contrast of 10^{-10} eventually. High precision of transmission should be able to be achieved by adopting the "measurement before coating" procedure. That is, for the coating of each step, a trial coating is performed on a blank substrate until the measurement shows that it meets the precision requirement, then the same procedure is applied on the pupil mask. Another concern regarding the transmission mask is the possible error of wave-front flatness. The thickness of the MCNDA coating is typically less than 10 nm (Omega Optical Inc. 2007, private communication), and for a step-transmission filter the wave-front flatness error over the entire pupil induced by the thickness differences between different steps is less than 1/10 waves in the visible. The absolute intensity variation in each transmission step at different wavelengths is relatively small. For example, the relative intensity variation over a wavelength range of 110 nm at a 550 nm design wavelength is between 0.1%–0.6%, which has a small influence on the high-contrast imaging (with contrast degradation less than 10^{-1}). Our stepped-transmission filters, realized by the MCNDA technique, have the potential for high-contrast imaging over a moderate wavelength range.

Although our discussion is focused on the mask that is composed of two filters, the mask that is composed of only one filter should also be addressed because of its high throughput. Figure 9 shows the PSF of a 21 stepped apodization pupil

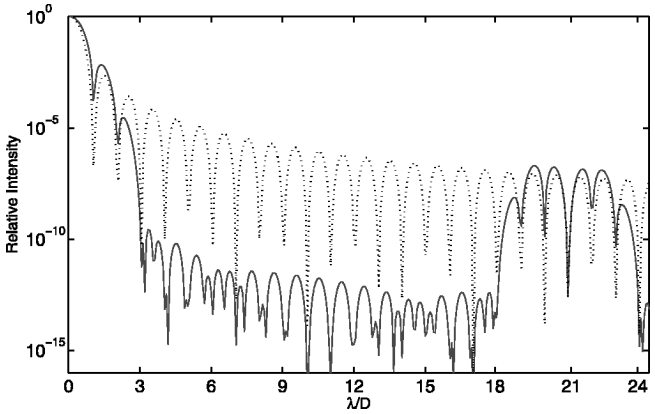

FIG. 10.—PSF section plot of 21 step one-filter apodization pupil (*solid line*). The dotted line shows the PSF of the squared pupil without apodization. The one-filter apodization pupil delivers a throughput of 30%. The plots are cut along the square diagonal direction.

composed of only one filter. The associated PSF section plot is shown in Figure 10. The one-filter apodization pupil delivers a transmission of 30% at the expense of a larger inner working angle that is $\sim 4\lambda/D$.

Filters with step number less than 21 can be commercially manufactured without difficulty. For example, a 21 step filter can be made with a size of 105 × 105 mm clear aperture, if each step is 5 mm wide (with a precision of better than 0.1 mm). Filters with step numbers significantly larger than 21 may result in a large filter size and are therefore difficult to make. The stepped-transmission technique, however, is not limited by the contrast issue, since high and ultrahigh contrast can be achieved by using filters with the same step number and same step width.

5. CONCLUSION

We have discussed a coronagraph that is based on two stepped-transmission filters. We show that the coronagraph can achieve high-contrast (10^{-10}) and ultra–high-contrast (10^{-14}) imaging at an angular distance larger than $(2–3)\lambda/D$ theoretically. For high-contrast imaging, the outer working angle is a function of the step number of the filters. Increasing the number of filter steps can increase the outer working angle. The ultra–high-contrast design allows the increasing of the discovery area or the accommodation of moderate manufacture error. The Airy throughput of the coronagraph achieves 99% against the total pupil throughput, which is an advantage for the reduction of scattered light for the planet detections in the zodiacal disk. The absolute transmission variation over different wavelengths for the filter is relatively small, which makes the coronagraph suitable for high-contrast imaging over a moderate wavelength range. The employment of stepped-transmission filters simplifies the manufacturing of the transmission pupil, making the transmission-based coronagraph suitable for high-contrast imaging in practice. Currently, we have two stepped-transmission filters being man-

ufactured which are designed for ultra–high-contrast imaging, and detailed results will be discussed in future publications.

We are grateful to Dr. Olivier Guyon, who has kindly provided detailed and helpful comments. Dr. Robert Vanderbei read this manuscript and provided helpful comments. We thank Angela Cookson for reading and correcting the manuscript. This work is supported by a grant provided by the Nanjing Institute of Astronomical Optics and Technology. Part of the work described in this paper was carried out at California State University, Northridge, with support from the National Science Foundation under grant AST 05-01743.

REFERENCES

Aime, C., Soummer, R., & Ferrari, A. 2002, A&A, 389, 334
Eberhard, A. 1973, IEEE Trans. Audio Electroacoustics, 21, 37
Enya, K., Tanaka, S., Abe, L., & Nakagawa, T. 2007, A&A, 461, 783
Gonsalves, R., & Nisenson, P. 2003, PASP, 115, 706
Guyon, O., Pluzhnik, E. A., Kuchner, M. J., Collins, B., & Ridgway, S. T. 2006, ApJS, 167, 81
Kasdin, N. J., Vanderbei, R. J., Spergel, D. N., & Littman, M. G. 2003, ApJ, 582, 1147
Nisenson, P., & Papaliolios, C. 2001, ApJ, 548, L201
Slepian, D. 1964, Bell Syst. Tech. J., 43, 3009
———. 1978, Bell Syst. Tech. J., 57, 1371
Vanderbei, R. J., Kasdin, N. J., & Spergel, D. N. 2004, ApJ, 615, 555
Verma, T., Bilbao, S., & Meng, T. H. Y. 1996, in IEEE International Conference on Acoustics, Speech, and Signal Processing (New York: IEEE), 1351